Accepted manuscript. Published in Rock Mechanics and Rock Engineering (2023). Version of record: https://doi.org/10.1007/s00603-023-03518-6. This version of the article has been accepted for publication, after peer review, and is subject to Springer Nature's AM terms of use, but is not the Version of Record and does not reflect post-acceptance improvements, or any corrections. The Version of Record is available online at: https://doi.org/10.1007/s00603-023-03518-6

Effect of relative humidity on the creep rate of rock salt at intermediate-low stresses

Yao Wang[a], Yida Zhang[a*]

[a] Department of Civil, Environmental and Architectural Engineering, University of Colorado, Boulder, CO 80309, USA

[*] Corresponding author: yida.zhang@colorado.edu

ABSTRACT

Understanding and accurately modeling the creep behavior of rock salt is of great interest for its relevance to geological storage of nuclear wastes, oil, and gases. Many experimental studies on the creep of salt samples are performed at a deviatoric stress above 5 MPa. The creep rates at smaller stress levels are usually estimated by extrapolating from data at higher stress levels. However, recent low-stress creep tests conducted at below 1 MPa suggest that such extrapolation can significantly underestimate the creep rate of rock salt, as the controlling micro-mechanisms are very different in low- and high-stress regimes. Meanwhile, field observations suggest that salt creep is accelerated under higher ambient relative humidity (i.e., the so-called Joffe effect). The effect of humidity on salt creep in the pressure-solution dominating low-stress regime is even less understood at present. In this context, we conducted a series of long-term creep tests at intermediate-low uniaxial stresses of 1, 3, and 5 MPa on Avery Island salt samples. In order to quantify the effect of moisture on salt creep, a combined triaxial cell and air circulation system is designed to permit control over the environmental humidity. Three relative humidity levels (33%, 55% and 77%) are selected and are achieved through the vapor equilibrium technique. Our study confirmed that the creep rate at low stress level is indeed higher than those extrapolated from high-stress creep tests. For the same deviatoric stress, higher ambient humidity produces faster steady-state creep rate of salt samples. Finally, a modified creep law that incorporates the humidity dependency is proposed and validated against the new experimental data.

Keywords: Rock salt; Relative humidity; Creep; Pressure solution; Strain rate

HIGHLIGHTS

- The influence of ambient humidity on creep behavior of rock salt at intermediate-low stress regime was experimentally investigated.
- A novel experimental setup was developed to provide stable humidity- and stress-control during long-term uniaxial creep tests.
- Humidity-dependent scaling functions inspired by existing water retention and adsorption models were introduced in the steady-state creep model for rock salt.

1. INTRODUCTION

Deep geological disposal is one of the most promising solutions for the permanent storage of high-level nuclear waste (HLW) (Birkholzer et al. 2012; Ewing et al. 2016). In this approach, a network of deep underground tunnels and placement spaces are excavated to host heat-emitting nuclear wastes isolated by an engineered barrier system. Among the different types of host rocks, salt formation is considered as a promising option given its high heat conductivity, extremely low permeability, and the ability to flow and heal overtime (Urai et al. 1986, Mansouri et al. 2018, Wang et al. 2021). In such a context, a thorough understanding of the rheological properties of salt becomes extremely important in evaluating the short-term stability and long-term evolution of salt-based deep disposal structures (Chan et al. 1998; Martin et al. 2015; von Berlepsch et al. 2016).

Polycrystalline halite rock (termed as rock salt) consists of halite grains with diameter between 0.1mm and several decimeters, containing impurities in solid solution and secondary minder phases and fluids that trapped in inclusions, grain boundary, or pores (Urai et al. 2008). As massive bodies of underground applications such as shafts storing nuclear wastes, the time-dependent closure process of rock salt is critical to ensure long-term environmental safety of the abandonment. At high deviatoric stress levels, rock salt deforms and fails through intergranular microcracking and salt grain movement. The time-dependent deformation in this regime is termed as dislocation creep, which is the dominant deformation mechanism of deep salt domes and described by a stress-dependent power-law model (Carter et al. 1983; Wawersik et al. 1986; Cornet et al. 2018). At low deviatoric stresses, another creep mechanism, namely the pressure solution creep, starts to gain dominance. This phenomenon is associated with water-activated solution-precipitation process, during which water dissolves salt at grain contacts and diffuses it away to precipitation sites (Cornet et al. 2018). Recent field and laboratory studies on rock salt confirmed that the actual creep rate at low-stress levels (< 1 MPa) is much higher than the creep rate extrapolated from the

high-stress regime data. For example, Bérest et al. (2005) performed a multistage uniaxial creep test at 0.1, 0.2, 0.3, and 0.5 MPa on Avery Island salt in a stable environment with temperature (T = 286.5 K) and relative humidity (RH = 72 ± 3%) provided by a 160-m-deep room in the Varangeville Mine in eastern France. They observed that the steady-state strain rate at a low axial stress of σ = 0.108 MPa achieves 1.4×10^{-12} s^{-1}, which is faster by 5 orders of magnitude than the extrapolated strain rate from high-stress range ($\dot{\varepsilon} = 10^{-17} s^{-1}$). This can be explained by the transition of dominant deformation mechanism from dislocation creep at high-stress level to pressure solution creep in low-stress range (Urai & Spiers 2007; Cornet et al. 2017; Gunther et al. 2015).

In addition to stress conditions, laboratory evidence has demonstrated that the presence of water can significantly modify the rheological behaviors of rock minerals by introducing dynamic recrystallization and promoting pressure solution creep (Chopra et al. 1984; Chen et al. 2006; Xu et al. 2013). Joffe et al. (1924) first suggested the effect of ambient humidity on the ductility of freshly cleaved halite specimens. This concept was then extended to refer to humidity effect on the mechanical behaviors of rock salt under constant load and temperature (Parker et al. 1958). Urai et al. (1986) observed a typical dislocation creep behavior on dry dilated salt while a marked weakening of brine-bearing samples at low strain rates, which demonstrates the necessity of considering the influence of trace amounts of brine on predicting the long-term evolution of rock salt. Besides laboratory measurements, Van Sambeek (2012) conducted a field observation and demonstrated the correlation between high relative humidity and the accelerated creep deformation of salt pillars and unlined shaft. At the vicinity of underground openings with low confining pressure, Hunsche et al. (1996) detected the accelerating effect of air humidity on the measurable creep deformation of rock salts, that is, a common humidity of 45% increases creep by a factor of about 5 compared to dry salt or undisturbed condition. It is conceivable that fluid films at grain-boundary can lead to dynamical recrystallization and enhance solution-transfer creep. Most of the existing

77 studies, however, discussed the Joffe's effect based on qualitative observations (Peach et al. 2001; Ter
78 Heege et al. 2005; Urai & Spiers 2007; Urai et al. 2008). Specifically, to the authors' knowledge, there is
79 no experimental data quantifying the potential impact of humidity on the low-stress creep behavior of rock
80 salt which is presumedly dominated by water-mediated pressure solution processes. These knowledge
81 gaps hinder a reliable prediction of long-term deformation of salt-based storage facilities accounting for
82 environmental variabilities.

83 In this context, this study explores the creep behavior of rock salt in intermediate-low stress domain
84 under various ambient relative humidity. A series of multistage uniaxial test was performed in an upgraded
85 triaxial cell on rock salt samples that were cored from the Avery Island mine in Louisiana, United States.
86 The applied stresses were in the 1-5 MPa range, while three different degrees of relative humidity (33%,
87 55%, and 77%) were considered. In the following, the testing program including the material, the
88 experimental setup, and the procedure is introduced (Section 2). The results are analyzed and discussed
89 (Section 3). Finally, an RH-dependent creep model is proposed and validated based on the present data
90 (Section 4).

91 **2. EXPERIMENTAL PROGRAM**

92 ***Specimen preparation***

93 The Avery Island salt samples in this study were provided by the RESPEC facility in Rapid City,
94 South Dakota. The Avery Island rock salt is dense, microcrystalline, opaque, white to light gray halite,
95 with only minor occurrences of other evaporite. The identified water-insoluble minerals in Avery Island
96 salt include limonite, pyrite, hauerite, dolomite, anhydrite calcite, quartz, Sulphur, hematite, and kaolinite.
97 One 15-inch by 22-inch core of Avery Island salt was first acquired through the Solution Mining Research
98 Institute (SMRI). The bulk core sample was then cut down to the desired sample height, and the standard
99 cylindrical specimens of 2 inch in diameter and 4 inch in height were subsequently extracted from these

bulk core samples. To reach the required flatness and parallelism of two ends, the surfaces and ends of these cylindrical specimens were grinded and polished. The samples were sealed and stored immediately after drilling and polishing. Thus, all samples shared similar physical properties, including the dimensions, weights, and initial moisture contents.

Experimental setup

A dead-weight loading frame (Karol-Warner CO.) with 1:11 lever ratio was used to perform the multistage uniaxial creep test. In order to investigate the effect of relative humidity, a triaxial cell was modified and assembled on the load frame to provide a sealed environment with controllable humidity, as shown in Fig. 1. Two glass discs were inserted between the loading platens and the sample to achieve the uniform distributed stress. The hemispherical end (the reaction point) of the loading frame was rested on the top of cell piston through a concaved connection which allows only the transmission of axial force to the piston. During the creep test, a high-resolution displacement sensor (Solartron linear encoder) with 0.5 μm accuracy and 0.0125 μm resolution was positioned at the top of the frame beam to register the axial displacement.

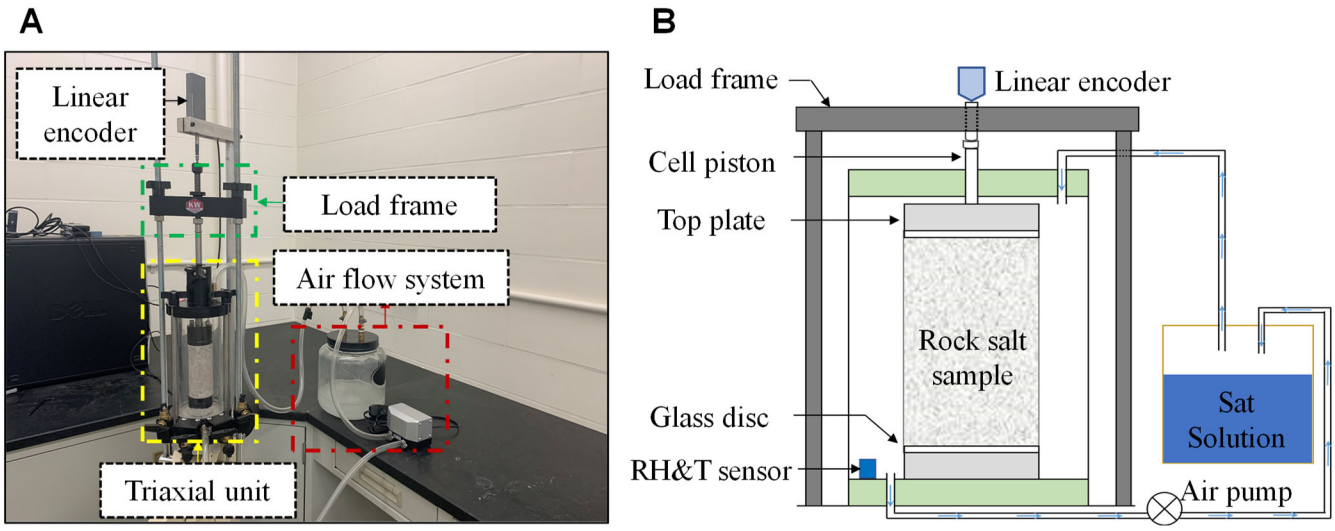

Fig. 1 RH-controlled uniaxial creep test: (A) Overview of the entire experimental setup; (B) Schematic of the RH control system.

Compared to the straightforward adjustment of creep stress, humidity control requires a closed space around the sample supplemented with a chemical system that can produce the desired equilibrium vapor pressure (Greenspan 1977). For example, each saturated electrolyte solution at given temperature offers a specific relative humidity, which is often used in the vapor equilibrium technique for stable humidity control in laboratory. In this study, we selected the saturated solutions of magnesium chloride ($MgCl_2$), magnesium nitrate ($Mg(NO_3)_2$), and sodium chloride (NaCl) in order to probe the creep response of rock salt under a wide range of RH values (Table 1). The saturated electrolyte solution is placed in a glass jar (the "reservoir") which is connected with the triaxial cell via 1/4" ID plastic tubes to form a closed environment. The reservoir only regulates the humidity of the air in this closed environment. It does not exchange mass with the triaxial cell in any other way nor have the possibility to contaminate the rock samples in the triaxial cell. An air pump with max flow rate of 285 GPH is installed to help accelerate the air circulation between the triaxial cell and the saturated solution reservoir, thus shortening the time for the system to reach humidity equilibrium. It should be noted that too small air flow cannot effectively accelerate the equilibrium progress while too fast air flow can cause the air pump to overheat. Thus, the approximate air flow rate should be determined by the inner diameter of the connected plastic tube, the total air volume in the internal closed space, and the pump performance. The environmental condition inside the triaxial cell is monitored by a wireless humidity and temperature (RH&T) sensor throughout the sample preparation and creep testing phases.

Table 1 Selected electrolyte solutions and the corresponding RH ranges.

Solute	Chemical formula	Solubility in water (gm/liter)	RH range (%)
Magnesium Chloride	$MgCl_2$	558	32-33
Magnesium Nitrate	$Mg(NO_3)_2$	736	53-55
Sodium Chloride	NaCl	360	75-77

Experimental procedure

First, salt specimen is mounted on the loading platen without a jacket, and the triaxial cell is assembled as shown in Fig. 1. Before launching the loading program, it is necessary to achieve humidity equilibrium between the triaxial cell and the solution reservoir by maintaining the internal air circulation. This can be judged by whether the RH reading reached a steady value according to the RH&T sensor. This process usually takes about 2 weeks up to one month, depending on the target RH level. Once done, the target creep stress is instantaneously applied to the sample by adding weights on the hanger attached at one end of the lever, and the encoder starts to record the changes of sample deformation every 5 minutes.

In this study, multistage creep tests are performed on the three salt samples under RH=33%, 55% and 77%, respectively. Each sample will be consecutively subjected to 1 MPa, 3 MPa, and 5 MPa stresses with the RH maintained. At each stress level, the sample is allowed to creep for a sufficiently long time to pass the initial transient stage (i.e., primary creep). When the sample reaches the apparent steady state (i.e., secondary creep) judged visually based on the overall displacement history, the test is either concluded or the next stress level is applied. Arguably, multistep loading could produce a cumulative damage in salt sample and thus register some history dependence in the measured creep response. Previous studies, however, suggest that the steady-state strain rate is quasi-independent of time and loading history and only depends on the current stress state (Lau 2004; Zhang 2016), which justifies the loading procedure selected in the present study.

Temperature compensation

This test was conducted in an isolated small testing room equipped with a standard HVAC system inside the Soil Mechanics Laboratory at the University of Colorado Boulder. The room temperature remains mostly stable but is not perfectly constant throughout our creep tests (the duration of which can be a few months). Record shows that the room temperature across seasons fluctuates between 22~25 °C,

which is not trivial. To study the impact of temperature variation on the test system, the salt sample is removed from the triaxial cell, and the piston is locked in place with everything else being the same as depicted in Fig. 1. The room temperature $T(t)$ and displacement $\delta(t)$ were recorded over the period of 300 hours, indicating a temperature variation ΔT of about 3 °C. The high-resolution displacement sensor correspondingly registered a displacement variation $\Delta\delta$ of about 13 μm, which is not negligible compared with the anticipated creep displacement of salt samples. We then calibrated the thermal corrector α of the system by enforcing $\Delta\delta(t) - \alpha\Delta T(t) \approx 0$. The calibrated α value for our system is 0.0039 [unit: mm/°C]. Obviously, α is dependent on the dimensions and the materials of the components of the testing device, and it is necessary to update this value for different experimental setups. From here on, all displacement data presented below are already corrected for the system's thermal deformation effect. Note that this correction will not eliminate the intrinsic temperature-dependent mechanical properties (i.e., thermoelasticity) of salt specimens. As a result, a 3 °C temperature fluctuation will still introduce some degree of uncertainty to the data obtained in this study. It would be ideal to perform the proposed experiments in a thermally stable underground space as done by Bérest and co-workers (Bérest et al. 2019) in future extensions of this work.

3. RESULTS AND DISCUSSIONS

Creep displacement

The displacement, RH, and temperature data for all three samples during the 3-stage creep tests are presented in Fig. 2. Each curve exhibits the standard elastic compression, transient creep, and steady state creep phases. In all three tests, the RH levels are maintained quite well, confirming the effectiveness of our vapor equilibrium setup. The temperature fluctuation is within the anticipated 3 °C throughout all tests. The displacement data from the RH=33% test exhibit slightly larger fluctuations compared to the other two, likely due to the relatively low displacement registered and the slightly larger temperature

variations experienced during the test. Comparing Figs. 2A, B and C, we observed that samples with higher RH develop larger cumulative displacement for less total creep time. This suggests a strong RH-dependent creep behavior at the stress levels tested in this study, which will be discussed in detail in the following sections.

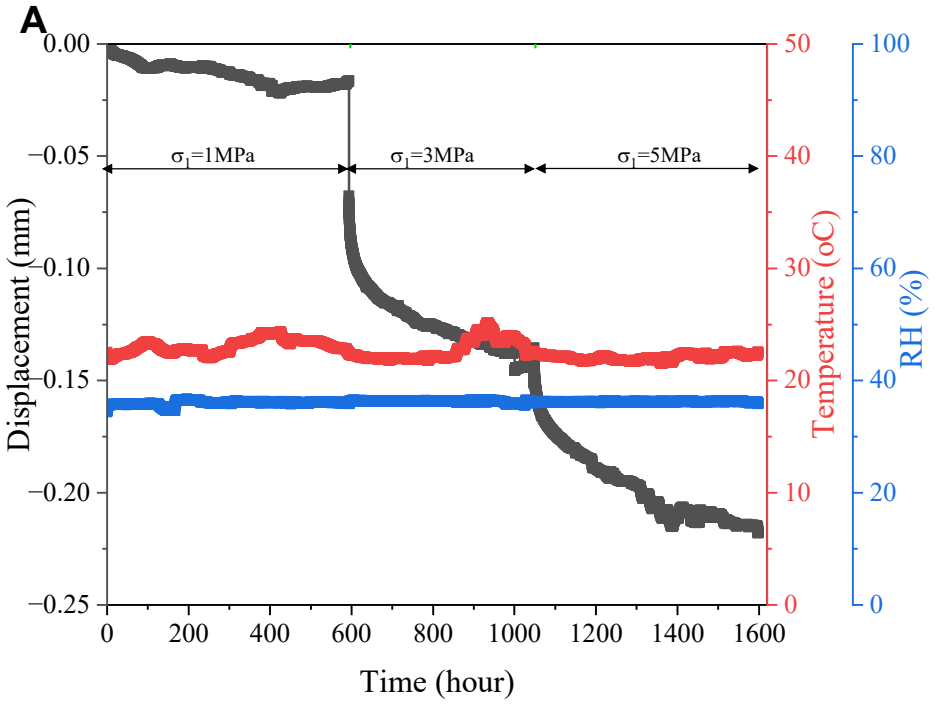

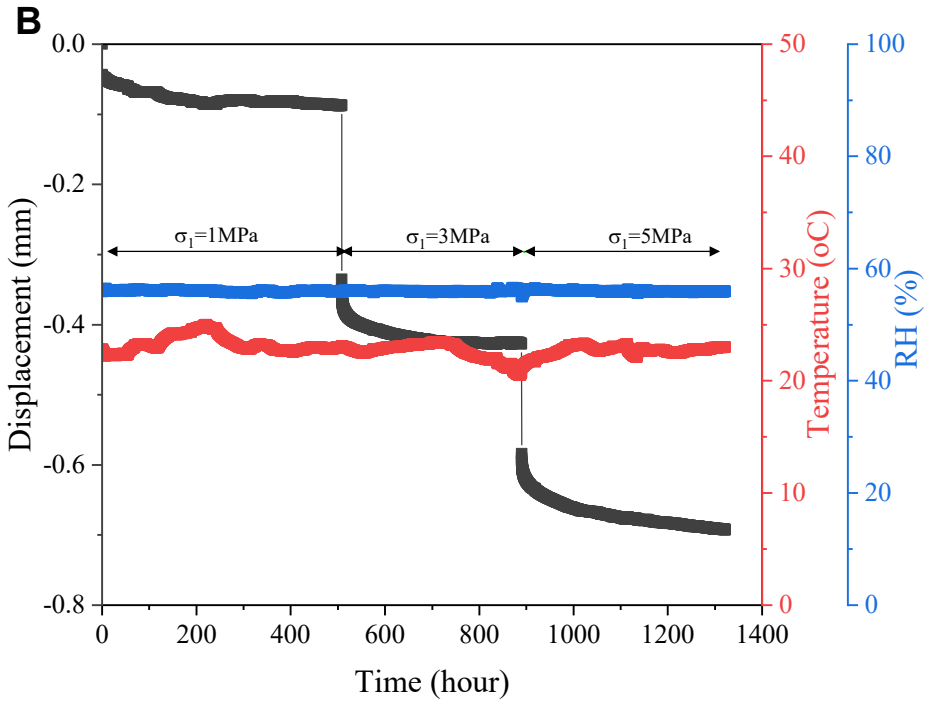

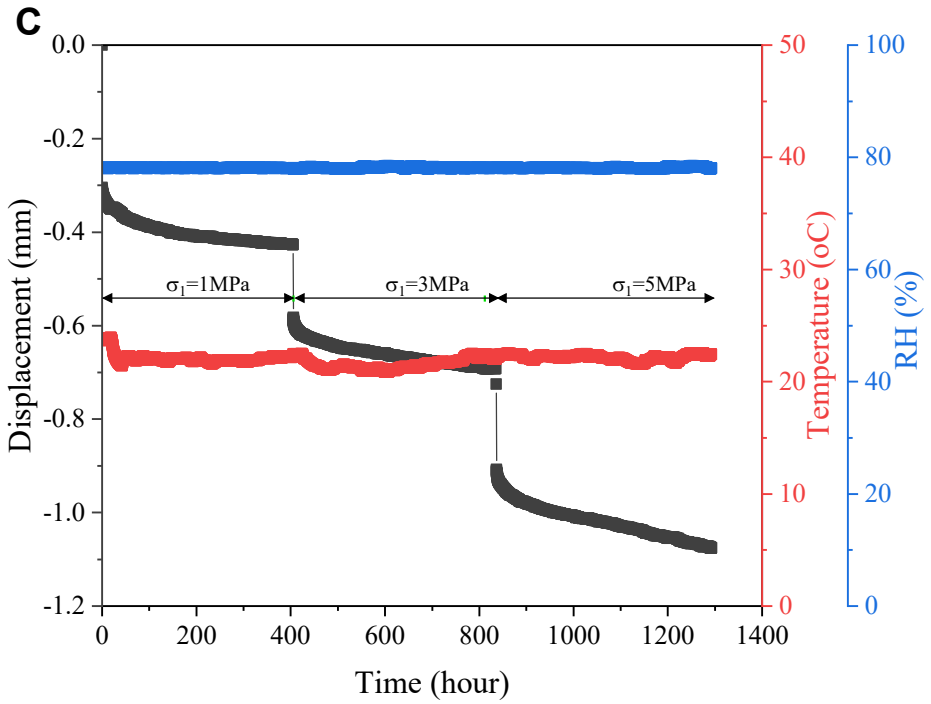

Fig. 2 Displacement, temperature, and RH data under different axial load (σ_1 =1, 3, and 5 MPa) and ambient humidity: (A) RH = 33%; (B) RH = 55%; (C) RH = 77%.

Creep strain and rate

The creep strains for 1 MPa, 3 MPa, and 5 MPa at different RHs are calculated based on the measured displacement and are plotted in Fig. 3A, C, and E, respectively. The strain data are then best fitted by a power law equation:

$$\varepsilon = a(t/t_0)^b \quad (1)$$

where t_0 is a reference time which is set to be 1 hour; a and b are two empirical parameters which vary with different environmental conditions (see Table 2). Note that the best-fit curves are shifted such that their initial points match the beginning of the corresponding loading segments (i.e., the moment of load application). The strain rate is calculated by taking the derivative of Eq. (1) with respect to time, and the results are plotted in Fig. 3B, D, and F for increasing stress levels at three different humidity degrees, respectively. It is observed that all tests have apparently reached a steady state at the end of the loading, although a slight decrease in strain rate would be expected should the test continue. In Fig. 3B, the strain rate of the 5 MPa case in the transient stage appears to be very close and even lower than the 3 MPa case. This could be attributed to the sequential nature of these creep tests: the transient creep for 5 MPa is dependent on the previous loading stage, where some perturbations in the displacement history (due to thermal fluctuations or external vibrations) can be seen at the end of the 3 MPa loading (Fig. 2A). These perturbations could have slightly altered the material microstructure and reduced the transient creep rate upon further loading. Overall, the steady-state creep rate clearly increases with respect to increased stress level for all RH levels.

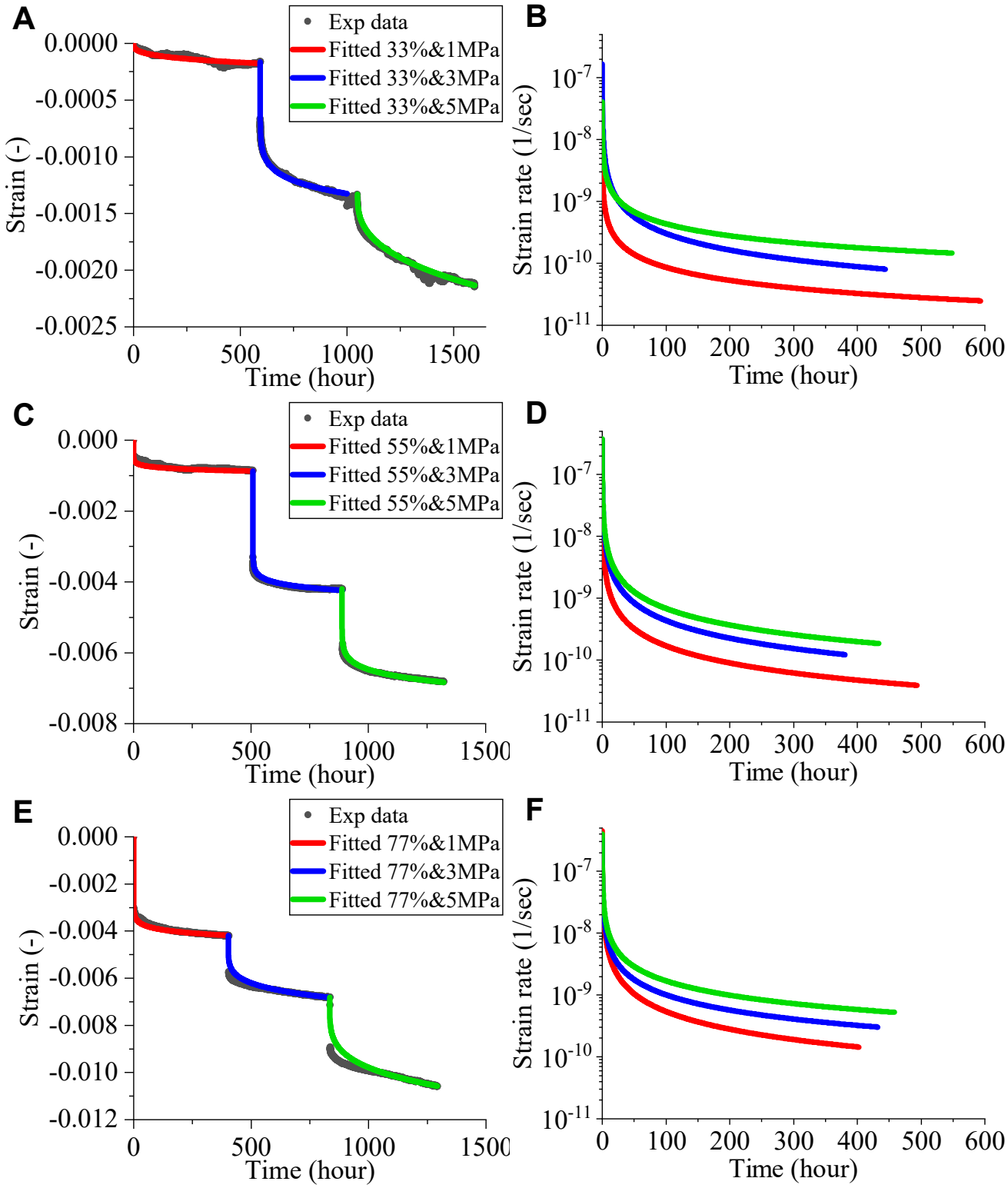

Fig. 3 Power-law fitting of the creep strain data (left column) and the calculated strain rate (right column) under different ambient humidity and applied stress (A&B = 33%RH; C&D = 55%RH; E&F = 77%RH)

Table 2 Best-fit parameters for Eq. (1)

RH	σ (MPa)	a (-)	b (-)
33%	1	-2.60×10^{-5}	0.30
	3	-6.00×10^{-4}	0.11
	5	-8.30×10^{-5}	0.36
55%	1	-5.30×10^{-4}	0.08
	3	-2.50×10^{-3}	0.05
	5	-1.35×10^{-3}	0.11
77%	1	-3.10×10^{-3}	0.05
	3	-8.80×10^{-4}	0.18
	5	-9.20×10^{-4}	0.23

To better visualize the effect of RH on creep, Fig. 4 summarizes the steady-state creep rates extracted at the end of each strain rate curves. It is apparent that RH has a major impact on the creep rate vs. stress curves in the tested stress range (1~5 MPa). For example, at 5 MPa axial stress, the steady-state strain rate of the sample under 77% relative humidity is about three times that of the sample under 55% RH and four times that of the sample under 33% RH. This may be conceptually explained as follows: When sufficient moisture is available in the environment, water molecules are preferably trapped (due to adsorption or condensation) at the points of increased energy, e.g., at sharp convex surfaces and at the stress concentrations like the contact points between grains, cracks, and pores. At these points, the solubility of salt is locally raised and forms a thin brine film. The mechanical energy produced by contact region between grains will be dissipated by in situ recrystallization, eventually promoting the so-called pressure solution creep. Conversely, less intergranular area will be filled by connected liquid films if the concentration of water vapor (or relative humidity) is low in the atmosphere, thus inhibiting the pressure solution creep at low deviatoric stresses (Fig. 5). Another mechanism, dislocation creep, can also contribute to the overall viscoelastic behavior of rock salt as shown in Fig. 5. But it is usually activated at high deviatoric stresses and is believed to be less dependent (if any) on ambient humidity. The strong RH dependency observed in our experiment suggests that pressure solution is still the dominating creep

mechanism at stress range of 1~5 MPa. Although not conclusive, one can see from Fig. 4 that the creep rate is more sensitive to RH at 1 MPa and becomes less affected by moisture changes at 5 MPa. This is consistent with our speculation that the RH dependency comes from the pressure solution creep which is more significant in low stress regime.

Overall, the steady-state creep strain rates obtained in this study (2×10^{-11}~5×10^{-10} /sec) for 1 ~ 5 MPa stress are orders of magnitude higher than the extrapolated values from the creep rate dataset obtained in high-stress regimes (5~20 MPa) for Avery Island Salt (see Fig. 2 in Bérest et al. (2015)). At each RH level, we note that the data appear to be quite linear on the log-log plot, as opposite to the bi-linear trend presented in Bérest et al (2019). This is likely because the selected stress range 1~5 MPa is not wide enough to encompass both the typical low-stress and the high-stress creep behavior. Future follow-up studies may extend to the high-stress regime (5~50 MPa) or to extremely low-stress regime (0.1~1 MPa) to better separate the effect of RH on different creep mechanisms.

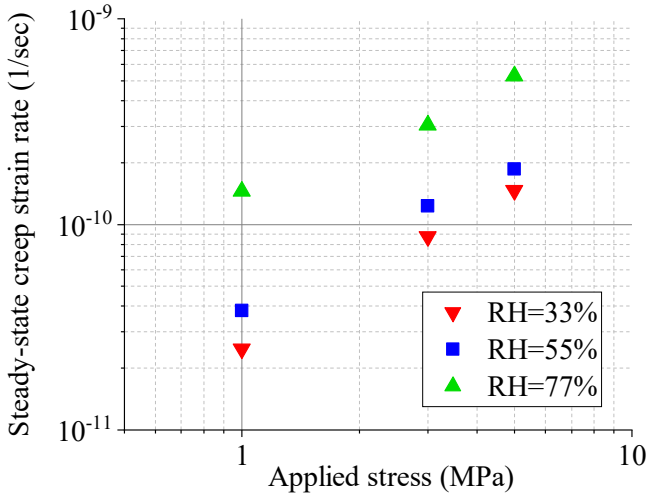

Fig.4 Steady-state creep rates of rock salts under different stress and humidity conditions

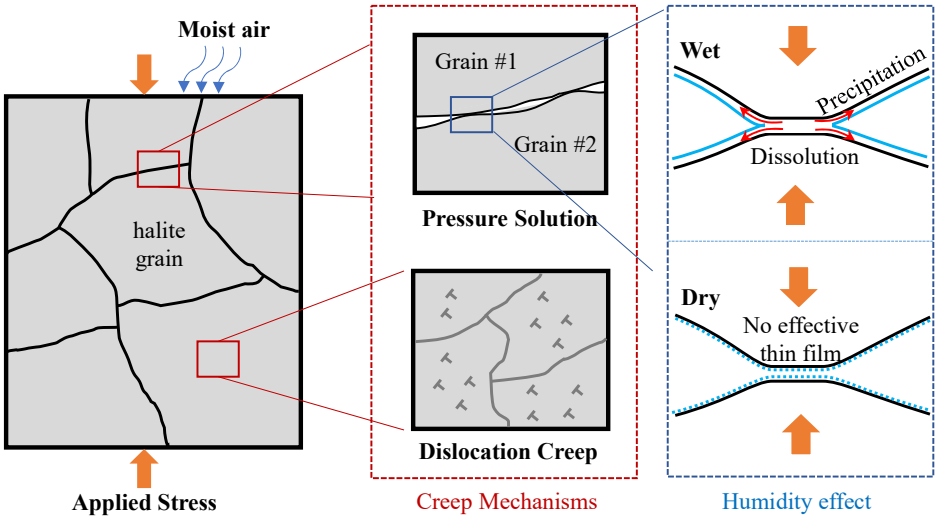

Fig. 5 Micromechanisms and the effect of humidity on salt creep

4. MOISTURE-DEPENDENT CREEP MODELING

Creep model

The steady-state creep of rock salt can be modelled by a combination of linear and power-law relationship that respectively indicate pressure solution creep and dislocation creep, based on experimental observations (Urai et al., 1986; Cristescu et al., 1988; Hunsche et al., 1999; Ter Heege et al.,2005)

$$\dot{\varepsilon} = \dot{\varepsilon}_{DC} + \dot{\varepsilon}_{PS} \tag{2}$$

The first term on the RHS represents dislocation creep using a Dorn-type power law equation (Ter Heege et al. 2005):

$$\dot{\varepsilon}_{DC} = A\, exp\left(-\frac{Q_{DC}}{RT}\right)\left(\frac{\sigma_1 - \sigma_3}{\sigma_0}\right)^n \tag{3}$$

The second term describes pressure solution creep by introducing a RH-dependent term into the original equation of Urai et al. (2007):

$$\dot{\varepsilon}_{PS} = B\Phi(RH)\, exp\left(-\frac{Q_{PS}}{RT}\right)\left(\frac{\sigma_1 - \sigma_3}{\sigma_0}\right) \tag{4}$$

where σ_0=1 MPa is a reference stress for normalization purpose; A and B are two material parameters that may depend on temperature and grain size; Q_{DC} and Q_{PS} are the activation energies for dislocation creep

and pressure solution creep, respectively; R is the ideal gas constant; T is absolute temperature; σ_1 and σ_3 are the maximum and minimum principal compressive stresses, respectively; n is the the power-law coefficients for dislocation creep. The proposed dimensionless function Φ(RH) represents the dependency of pressure solution creep rate on the relative humidity. We suspect that Φ is physically related to the thickness of the water film between the grains based on the conceptualization in Fig. 5. Without direct experimental data quantifying the film thickness, here we will treat Φ just as a phenomenological scaling function to be calibrated by our experimental data.

Considering isothermal and uniaxial stress condition adopted in this study, Eqs. (2)-(4) can be simplified to

$$\dot{\varepsilon} = a_1(\sigma/\sigma_0)^n + a_2\Phi(RH)(\sigma/\sigma_0) \quad (5)$$

where a_1 and a_2 are material parameters responsible for dislocation creep and pressure solution creep, respectively; σ is the deviatoric stress which equals to σ_1 in uniaxial compression; similar with Eq. (3), σ_0=1 MPa is a reference stress for normalization purpose.

Model calibration

Fig. 6 plots Eq. (6) fitted to the data obtained from our creep tests. Note that the same values of n, a_1, and a_2 parameters with only Φ varying are used to capture the creep rate data at different RH levels. One can see that the model performs quite well overall. All curves are essentially the depiction of the second term in Eq. (5), as the value of coefficient a_1 is orders of magnitude smaller than a_2. In other words, the $\dot{\varepsilon} - \sigma$ data at each RH level mostly follow a quasi-linear relation, indicating the dominance of pressure solution creep in the tested stress range. The dislocation creep coefficient n is arbitrarily set to 3 in Fig. 6, as a more reliable calibration of n requires creep rate data at higher stresses.

It is worth noting that the model underpredicts the creep rate for RH=77% at 1 MPa but not for the other two RH levels. This suggests a deviation of the creep rate trend from the linear $\dot{\varepsilon} \propto \sigma$ line that corresponds to pressure-solution creep. Noticing that RH=77% is exactly the equilibrium RH for saturated

NaCl solutions, we speculate that other chemical processes may have dominated the creep rate at this particular RH in the low stress domain. In early pilot tests, we have tried to use pure water in the reservoir to generate a RH=100% environment for the creep testing. It turned out that rock salt which is mostly NaCl cannot maintain chemical stability in such an environment even if no stress is supplied, as excessive water will be drawn from the atmosphere to "melt" the specimen in a short period of time. Afterall, the relative humidity of the air in equilibrium with a saturated NaCl solution is 77%. In this vein, a tiny fluctuation of RH around 77% or a deviation of the composition of rock salt from pure NaCl may introduce non-trivial chemical perturbations to the rock salt samples. Such speculation, however, may only be tested or validated after performing more creep tests at RH=77% for stresses below 1 MPa.

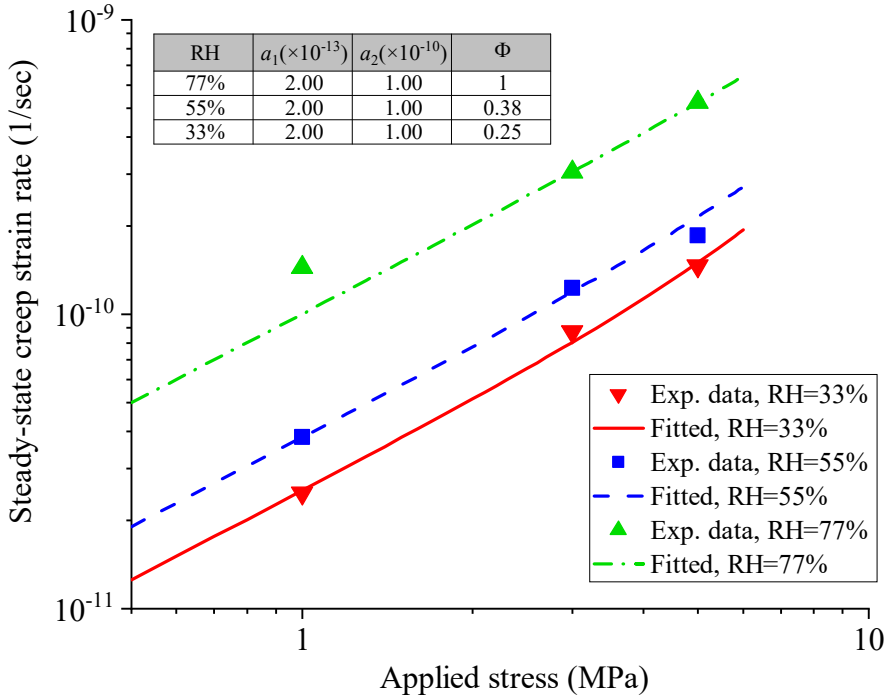

Fig. 6 Measured vs. modeled steady-state strain rate. The units of a_1 and a_2 are 1/sec.

RH dependency

The calibration in Fig. 6 suggests that the Φ monotonically increases with respect to RH. Based on the hypothesis that Φ is correlated with the amount of water retained in the salt matrix, we expect that the expression of Φ takes similar form as existing water retention models or water adsorption isotherms.

One such equation is the van Genuchten (1980) model which is commonly used to describe the relationship between the water content and the suction in unsaturated soils (Wild et al. 2015, Zhai et al. 2017, Espitia et al. 2019). The following Φ expression is proposed inspired by the van Genuchten (VG) model:

$$\Phi = \frac{1}{\left[1 + \left(\chi(\psi - \psi_0)\right)^{\kappa}\right]^{1-\frac{1}{\kappa}}} \tag{6}$$

where χ and κ are model parameters; ψ is the total suction; ψ_0 is the reference suction value at $RH_0 = 77\%$. The reason to introduce ψ_0 is to ensure that Eq. (6) satisfies $\Phi = 1$ at $RH_0 = 77\%$. As discussed earlier, rock salt cannot maintain chemical stability for RH > 77%, for which Eq. (6) should be only used for $RH \in [0\%, 77\%]$. The scaling factor Φ is thus set to 1 at RH = 77% as a matter of convenience.

To relate suction with relative humidity, the Kelvin's law is invoked (Butt et al. 2013):

$$\psi = -\frac{\rho_l RT}{M_l} ln(\mathrm{RH}) \tag{7}$$

where ρ_l and M_l are respectively the liquid water density (1000 kg/m^3) and molar mass (18.016 g/mol); R is the constant ideal gas (8.31432 J/[mol K]) and T is the room temperature in this study (296 K). According to Eq. (7), the calculated reference suction ψ_0 is 35 MPa at RH = 77%.

Another plausible model for Φ is the Brunauer-Emmett-Teller (BET) isotherm. The BET isotherm describes the multilayer-adsorption of gas species on a free solid surface (Brunauer et al. 1938) and is also used to calculate the effective surface area of porous materials based on adsorption data (Gelb et al. 1998). An expression of Φ inspired by the BET isotherm can be proposed as:

$$\Phi = \frac{(1 - RH_0)(1 + RH_0(c-1))}{(1 - RH)(1 + RH(c-1))} = \frac{0.23(1 + 0.77(c-1))}{(1 - RH)(1 + RH(c-1))} \tag{8}$$

in which c is the only model constant. It is easily shown that Eq. (8) also satisfies $\Phi=1$ at $RH_0=77\%$, similar to Eq. (6).

The performances of Eqs. (6) and (8) are shown Fig. 7. For both curves, portions with RH > 77% are truncated as they do not have any physical meanings. It is observed that both curves satisfy $\Phi=0$ at $RH_0=0\%$, which is desirable as pressure solution creep cannot occur if the environment contains no water molecules. One can see that the VG-based model (Eq. (6)) exhibits an overall better agreement with the data compared to the BET-based model (Eq. (8)). This is not surprising as the former contains two parameters, while the latter only has one. Therefore, Eq. (6) is recommended for describing the dependency of the steady-state creep rate of rock salt on the ambient humidity.

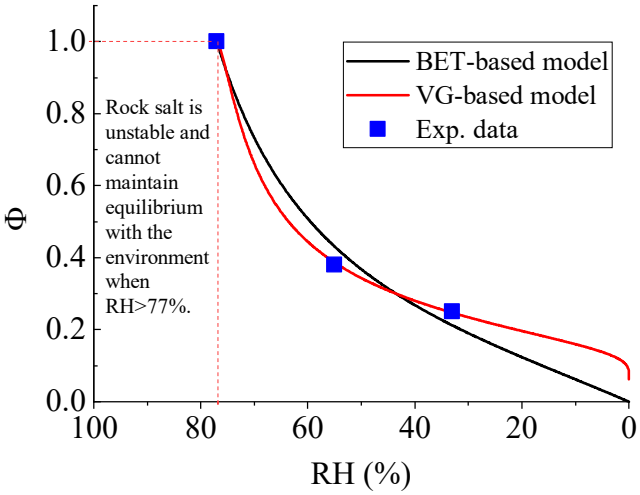

Fig. 7 Data vs. Φ functions based on VG and BET models. The best-fit parameters are: $\chi = 0.14$ 1/MPa, $\kappa = 1.5$, $c = 2.5$.

Finally, combining Eqs. (5)-(7), the creep rate – stress – RH surface for Avery Island salt is plotted in Fig. 8. The experimental data is satisfactorily captured by the proposed RH-dependent creep model for the current stress and RH ranges. The validity of the model could be further examined by obtaining and comparing with more creep data within and beyond the plotted stress and RH ranges. As we learned from recent studies on salt rock creep (Bérest et al., 2019), extra caution must be used when extrapolating the creep rate beyond known conditions.

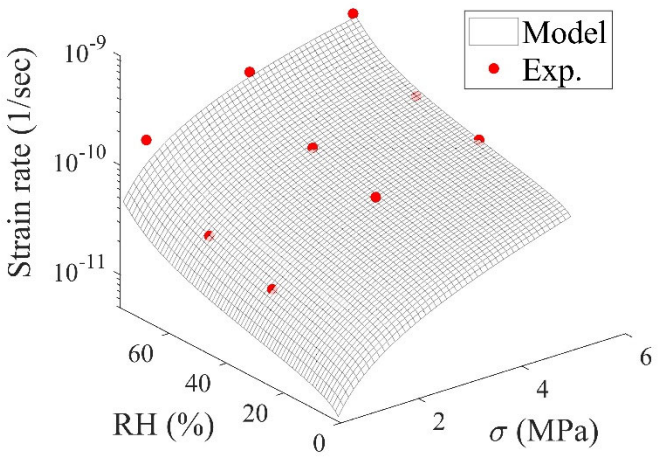

Fig. 8 Modeled vs. measured steady-state creep rate with respect to uniaxial stress and ambient humidity.

5. CONCLUSIONS

This paper reports the result of a laboratory study on the effect of ambient humidity on rock salt creep behaviors in intermediate-low stress regime, based on which a revised steady-state creep law is proposed to introduce RH-dependency in the pressure solution term. The main conclusions are highlighted below:

1) A novel experimental setup is designed to permit reliable relative humidity control during dead-load uniaxial creep tests. The humidity control is realized through vapor equilibrium technique combined with a modified triaxial cell.
2) Our study confirms that, at intermediate-low stress regime (1-5 MPa), the creep response is significantly affected by the relative humidity of the environment.
3) The effect of moisture is slightly enhanced at lower deviatoric stresses, although the trend is not decisive. This may suggest that pressure solution creep gains dominance over dislocation creep at low stress levels. As the RH sensitivity reduces at higher stresses (e.g., 5 MPa), it is plausible that dislocation creep is less dependent on the ambient humidity as compared to pressure solution creep.

4) We introduced a dimensionless function Φ in a steady-state creep law to scale the creep rate with respect to relative humidity. By hypothesizing that such scaling is proportional to the amount of liquid water available in the salt matrix, we proposed two Φ functions inspired by the van Genuchten water retention model and the Brunauer-Emmett-Teller adsorption isotherm. It is found that the two-parameter VG-based model can fit the experimental data quite well.

As a first study, the present experimental setup and experimental campaign can be further improved or upgraded in several aspects. First, the temperature control provided by the HVAC system of the testing room is not perfect. It will be ideal to perform the proposed experiments in a thermally stable underground space (e.g., Bérest et al. 2019) in order to completely eliminate the effect of temperature change on both the testing system and the material behavior. Second, due to the limited duration of the project, we were not able to probe the effect of RH on salt creep at extremely low deviatoric stresses (0.1~1 MPa) which are expected to last for a few years to reach steady state. Performing the proposed tests at wider stress ranges is desirable to allow one to identify the dual-regime creep behavior as reported in recent literatures (Baumann et al. 2022; Yang et al. 2021; Zha et al. 2021). These experiments will also help investigate the cause of the higher-than-expected creep rate at RH=77% at low stress levels. Finally, more experimental data is needed to further validate the proposed Φ function especially at lower RH levels. RH-controlled creep tests equipped with microstructural observations is desired to examine the mechanistic linkage between Φ and the amount of adsorbed water or water film thickness at grain boundaries.

6. ACKNOWLEDGEMENTS

This work was supported by the U.S. Department of Energy through grant DE NE0008771 and the Predictive Science Academic Alliance Program (PSAAP) under Award Number DE-NA0003962.

7. STATEMENTS AND DECLARATIONS

Conflict of Interest The authors have no financial or proprietary interests in any material discussed in this article.

REFERENECES

Baumann, T.S., Bérest, P., Brouard, B., ter Braack, M., den Hartogh, M., Kaus, B.J., Klaver, J., Oonk, P.B., Popov, A., Schmatz, J. and Urai, J.L. (2022) CCC-integrated multiscale study of salt cavern abandonment in the Netherlands.

Bérest, P., Blum, P., Charpentier, J., Gharbi, H., Vales, F. (2005) Very slow creep tests on rock samples. *International Journal of Rock Mechanics & Mining Sciences*, 42, 569-576.

Bérest, P., Beraud, J., Gharbi, H., Brouard, B., DeVries, K. (2015) A Very Slow Creep Test on an Avery Island Salt Sample. *Rock Mech Rock Eng*, 48, 2591-2602.

Bérest, P., Gharbi, H., Brouard, B., Bruckner, D., DeVries, K., Hevin, G., Hofer, G., Spiers, C., Urai, J. (2019) Very slow creep tests on salt samples. *Rock Mech Rock Eng*, 52, 2917-2934.

Birkholzer, J., Houseworth, J. and Tsang, C.F. (2012) Geologic disposal of high-level radioactive waste: Status, key issues, and trends. *Annual Review of Environment and Resources*, 37, pp.79-106.

Burnauer S., Emmett, P.H., Teller E. (1938) Adsorption of Gases in Multimolecular Layers. *Journal of the American Chemical Society*, 60(2), 309-319.

Butt, H.J., Graf, K. and Kappl, M. (2013) Physics and chemistry of interfaces. *John Wiley & Sons*.

Carter, N.L., Hansen, F.D. (1983) Creep of rock salt. *Tectonophysics*, 92(4), 275-333.

Chan, K.S., Bodner, S.R. and Munson, D.E. (1998) Recovery and healing of damage in WIPP salt. *International Journal of Damage Mechanics*, 7(2), 143-166.

Chen, S., Hiraga, T., and Kohlstedt, D. L. (2006) Water weakening of clinopyroxene in the dislocation creep regime. *Journal of Geophysical Research*, 111, B08203.

Chopra, P. N., and Paterson, M. S. (1984) The role of water in the deformation of dunite. *Journal of Geophysical Research*, 89(B9), 7861–7876.

Cornet JS, Dabrowski M, Schmid DW. (2017) Long-term cavity closure in non-linear rocks. *Geo J Int*, 210:1231–1243.

Cornet JS, Dabrowski M, Schmid DW. (2018) Long-term creep closure of slat cavities. *International Journal of Rock Mechanics and Mining Sciences*, 103, 96-106.

Cristescu, ND. (1998) Evolution of damage in rock salt. In: Mechanical behavior of salt. *Trans Tech Publications, Series on Rock and Soil Mechanics, Clausthal-Zellerfeld*, vol.22, 131-142.

Cristescu, ND., Hunsche, U. (1998) Time effects in rock mechanics. *Series: materials, modeling and compution, Wiley, Chichester*.

Espitia, J., Caicedo, B., Vallejo, L. (2019) Comparison of the uniaxial compressive strength of the Belencito claystone under stress control and suction control paths. *Rock Mechanics and Rock Engineering*, 19-34, 52(1).

Ewing, R.C., Whittleston, R.A. and Yardley, B.W. (2016) Geological disposal of nuclear waste: a primer. *Elements*, 12(4), 233-237.

Gelb, L., Gubbins, K. (1998) Characterization of Porous Glasses: Simulation Models, Adsorption Isotherms, and the Brunauer-Emmett-Teller Analysis Method. *Langmuir*, 14, 2097-2111.

Greenspan, L. (1997) Humidity fixed points of binary saturated aqueous solutions. *Journal of Research of the National Bureau of Standards*, vol.81.

Gunther, R., Salzer, K., Popp, T., Ludeling, C. (2015) Steady-State Creep of Rock Salt: Improved Approaches for Lab Determination and Modelling. *Rock Mech Rock Eng*, 48: 2603-2613.

Hunsche, U., Hampel, A. (1999) Rock salt – the mechanical properties of the host rock material for a radioactive waste repository. *Eng Geol*, 52(3): 271-291.

Hunsche, U., Schultze, O. (1996) Effect of humidity and confining pressure on creep of rock salt. *In: Hardy HR Jr, Langer M (eds) Proceedings of the third conference on the mechanical behavior of slat. Trans Tech Publications, Clausthal, Germany,* pp: 237-248.

Joffe, A., Kirpitschewa, M., Lewitsky, M. (1924) Deformation and strength of crystals, *Z. Physik*, 22:286.

Lau, J., Chandler, N. (2004) Innovative laboratory testing. *Int J Rock Mech Min Sci*, 1(8), 1427-1445.

Li, S., Urai, J. (2016) Rheology of rock salt for salt tectonics modeling. *Petroleum Science*, 13, 712-724.

Liu, Z., Xie, S., Shao, J., Conil, N. (2015) Effects of deviatoric stress and structural anisotropy on compressive creep behavior of a clayey rock. *Applied Clay Science*, 114, 491-496.

Mansouri, H., Ajalloeian, R. (2018) Mechanical behvaior of salt rock under uniaxial compression and creep tests. *International Journal of Rock Mechanics and Mining Sciences*, 220, 19-27.

Martin, L.B., Rutqvist, J. and Birkholzer, J.T. (2015) Long-term modeling of the thermal–hydraulic–mechanical response of a generic salt repository for heat-generating nuclear waste. *Engineering geology*, 193, pp.198-211.

Osses, R., Majdanishabestari, K., Ovalle, C., Pineda, J. (2021) Testing and modelling total suction effects on compressibility and creep of crushable granular material. *Science Direct*, 61, 1581-1596.

Parker, E., Pask, J., Washburn, J., Gorum, A., Luhman, W. (1958) Ductile ceramics – a high temperature possibility. *Journal of the American Ceramics Society*, p.161.

Peach, C., Spiers, C. (1996) Influence of crystal plastic deformation on dilatancy and permeability development in synthetic salt rock. *Tectonophysics*, vol. 256, 101-128.

Peach, C., Spiers, C., Trimby, P. (2001) Effect of confining pressure on dilatation, recrystallization, and flow of rock salt at 150oC. *J Geo Res Solid Earth*, 106, 13315:13328.

Ter Heege, J., De Bresser, J., Spiers, C. (2005) Rheological behavior of synthetic rock salt: the interplay between water, dynamic, recrystallization and deformation mechanisms. *J Struct Geo*, 27, 948-963.

Ter Heege, J., De Bresser, J., Spiers, C. (2005) Dynamic recrystallization of wet synthetic polycrystalline halite: dependence of grain size distribution on flow stress, temperature, and strain. *Tectonophysics*, 396, 35-57.

Urai, J., Spiers, C., Zwart, H., Lister, G. (1986) Weakening of rock salt by water during long-term creep. *Nature*, vol.324.

Urai, J., Spiers, C. (2007) The effect of grain boundary water on deformation mechanisms and rheology of rock salt during long-term deformation. *Proceedings of the 6th conference on the mechanical behavior of slat, Hannover, Germany*.

Urai, J., Schleder, Z., Spiers, C., Kukla, P., Lange, J., Rohling, H. (2008) Flow and transport properties of salt rocks. *In: Littke R, Bayer U, Gajewski D, Nelskamp S (eds) Dynamics of complex intracontinental basins: the central European basin system. Springers, Berlin*, pp: 277-290.

Van Genuchten, M.T. (1980) A close from equation predicting the hydraulic conductivity of unsaturated soil. *Soil Sci. Soc. Am. J.*, 44, 892-898.

Van Sambeek, L.L. (2012) Measurements of humidity-enhanced salt creep in salt mines: proving the Joffe effect. *Mechanical Behavior of Salt VII*, pp.179-184.

von Berlepsch, T. and Haverkamp, B. (2016) Salt as a host rock for the geological repository for nuclear waste. *Elements*, 12(4), 257-262.

Wang, J., Zhang, Q., Song, Z., Zhang, Y. (2021) Experimental study on creep properties of salt rock under long-period cyclic loading. *International Journal of Fatigue*, 143.

Wawersik, W.R., Zeuch, D.H. (1986) Modeling and mechanistic interpretation of creep of rock salt below 200 oC. *Tectonophysics*, 121(2), 125-152.

Wild, K., Barla, M., Turinetti, G., Amann, F. (2017) A multi-stage triaxial testing procedure for low permeable geomaterials applied to Opalinus Clay. *Journal of Rock Mechanic and Geotechnical Engineering*, 9, 519-530.

Wild, K., Wymann, L., Zimmer, S. (2015) Water retention characteristics and state-dependent mechanical and petro-physical properties of a clay shale. *Rock Mech Rock Eng*, 427-439, 48(2)

Xu, L., Mei, S., Dixon, N., Jin, Z., Suzuki, A. M., and Kohlstedt, D. L. (2013) Effect of water on rheological properties of garnet at high temperatures and pressures. *Earth and Planetary Science Letters*, 379, 158–165.

Yang, Lei, Jie Mei, Xiangchao Sheng, Weimin Yang, and Jinglong Li. (2021) Cracking and creep behavior of rocks considering propagation and interaction of adjacent cracks under hydro-mechanical coupling. *Rock Mechanics and Rock Engineering*, 54(8): 4099-4110.

Zha E, Zhang Z, Zhang R, Wu S, Li C, Ren L, Gao M, Zhou J. (2021) Long-term mechanical and acoustic emission characteristics of creep in deeply buried jinping marble considering excavation disturbance. *International Journal of Rock Mechanics and Mining Sciences*, 139: 104603.

Zhang, Y., Shao, J., Xu, W., Jia, Y. (2016) Time-dependent behavior of Cataclastic rocks in a multi-loading triaxial creep test. *Rock Mech Rock Eng*, 49, 3793-3803.

Zhai, Q., Rahardjo, H., Satyanago, A. (2017) Effects of residual suction and residual water content on the estimation of permeability function. *Geoderma*, 303, 165-177.